Structural Characterization of Fatty Acid Anions via Gas-Phase Charge Inversion Using Mg(tri-butyl-terpyridine)$_2^{2+}$ Reagent Ions

Sarah T. Nsiah, Kimberly C. Fabijanczuk, and Scott A. McLuckey*

Department of Chemistry

Purdue University

560 Oval Drive, West Lafayette, IN, United States, 47907-2084, USA

Short title: Fatty Acid Anion Charge Inversion with Mg(ttb-Terpy)$_2^{2+}$

*Correspondence:
Dr. Scott A. McLuckey
560 Oval Drive
Department of Chemistry
Purdue University
West Lafayette, IN 47907-2084, USA
E-mail: mcluckey@purdue.edu

ABSTRACT

RATIONALE

Free fatty acids (FFAs) and lipid classes containing fatty acid esters (FAEs) are major components of the lipidome. In the absence of a chemical derivatization step, fatty acid anions do not yield all of the structural information that may be of interest under commonly used collision-induced dissociation (CID) conditions. A line of work that avoids condensed-phase derivatization takes advantage of gas-phase ion/ion chemistry to charge invert fatty acid anions to an ion-type that provides the structural information of interest using conventional CID. This work is motivated by the potential for significant improvement in the overall efficiency for generating fatty acid chain structural information.

METHODS

A hybrid triple quadrupole/linear ion trap tandem mass spectrometer that has been modified to enable the execution of ion/ion reaction experiments has been used evaluate the use of 4,4′,4″-tri-tert-butyl-2,2′:6′,2″-terpyridine (ttb-Terpy) as the ligand in divalent magnesium complexes for charge inversion of fatty acid anions.

RESULTS

$Mg(ttb\text{-}Terpy)_2^{2+}$ complexes provide significantly improved efficiency in generating structurally informative products from fatty acid ions relative to $Mg(Terpy)_2^{2+}$ complexes, as demonstrated for straight-chain fatty acids, branched-chain fatty acids, unsaturated fatty acids, and cyclopropane-containing fatty acids. It was discovered that most of the structurally informative fragmentation from $[FA\text{-}H+Mg(ttb\text{-}Terpy)]^+$ arises from loss of a methyl radical from the ligand followed by radical-directed dissociation (RDD), which stands in contrast with the charge remote fragmentation (CRF) believed to be operative with the $[FA\text{-}H+Mg(Terpy)]^+$ ions.

CONCLUSIONS

This work demonstrates that a large fraction of product ions from the CID of ions of the form $[FA\text{-}H+Mg(ttb\text{-}Terpy)]^+$ are derived from RDD of the fatty acid backbone with a very minor fraction arising from structurally uninformative dissociation channels. This ligand provides an alternative to previously used ligands for the structural characterization of fatty acids via CRF.

Keywords: Divalent metal-ligand complexes, tri-tert butyl terpyridine, lipids, charge inversion

1. INTRODUCTION

Lipids that contain fatty acid esters (FAEs), such as glycerophospholipids (GPLs), as well as free fatty acids (FFAs) are essential components of the lipidome and play important roles in various biological processes, such as in signaling and membrane formation.[1] While FFAs have long been analyzed by derivatization to fatty acid methyl esters followed by gas-chromatography/mass spectrometry (GC/MS) or GC-tandem mass spectrometry (GC-MS/MS)[2,3,4,5] the advent of electrospray ionization (ESI) has greatly expanded the range of lipid classes amenable to MS and has since become the dominant ionization method in lipidomics.[6,7,8,9,10] Either applied directly to a lipid mixture, as in shot-gun lipidomics, [11,12,13] or in combination with liquid chromatography, ESI-MS/MS has become a major tool in characterizing the lipidome. [14] As lipidomics has evolved, the complete characterization of lipid structures has become a common objective. In the cases of FAEs and FFAs, for example, variations in chain length, degree and location of unsaturation, degree and location of branching, chain modifications, etc. are common and can be highly biologically relevant. For example, the identification and quantitation of double bond location on fatty acids can distinguish human lung cancer tissues from normal tissues.[15] In general, fatty acid ions, either generated directly from FFAs or via fragmentation of a FAE-containing ion, are most readily formed in the negative ion mode, which, via mass measurement, provides carbon number and degree of unsaturation. However, tandem mass spectrometry of deprotonated fatty acids using conventional collision-induced dissociation (CID) generally provides little structural information. For this reason, alternate dissociation methods[16,17,18,19,20,21,22] and/or condensed-phase derivatization reactions, [23,24,25,26,27,28] have been applied to generate the information of interest.

A particularly noteworthy strategy for the characterization of fatty acids is often referred to as 'charge switching'.[29] Charge switching approaches usually involve derivatization reactions, such as derivatization with pyridinium-containing reagents,[30,31,32,33,34] and/or the use of solution conditions amenable to the generation of cations via complex formation[35] for subsequent MS and MS/MS. However, condensed-phase derivatization strategies are not applicable to fatty acid anions generated via gas-phase fragmentation of a larger lipid, such as a GPL anion. An alternative strategy to effect charge switching of product anions generated via CID is to charge-invert them via a gas-phase ion/ion reaction using multiply-charged reagent cations. To this end, we have described the use of divalent alkaline earth metals, primarily Mg^{2+}, complexed with either 1,10-phenanthroline (Phen)[36,37] or 2,2':6',2"-terpyridine (Terpy)[38] ligands as charge inversion reagents for lipid anions. The overall process for a deprotonated fatty acid, described further below, results in a cation of the type $[(FA-H) + Mg(L)]^+$, where L is the ligand. This ion type has been shown generate fragment ions that reveal the location(s) of double bond(s),[39] cyclopropane moieties,[40] and the location of branching sites.[41] A recent review describes a wide variety of applications of gas-phase charge inversion for the structural characterization of various lipid classes.[42]

The original gas-phase charge inversion work using divalent metal complexes employed $Mg(Phen)_3^{2+}$ as the reagent ion. With this reagent, the loss of two Phen ligands is required to generate the $[(FA-H)+Mg(Phen)]^+$ ion that yields structurally informative product ions upon CID. We subsequently turned to $Mg(Terpy)_2^{2+}$ as the reagent ion because one less ligand loss step is required to generate the $[(FA-H)+Mg(Terpy)]^+$ ion. The $[(FA-H)+Mg(Phen)]^+$ and $[(FA-H)+Mg(Terpy)]^+$ ions show very similar dissociation behaviors. Since both ligands are commercially available and the Terpy-containing complexes require one less ligand loss, $Mg(Terpy)_2^{2+}$ is preferred over $Mg(Phen)_3^{2+}$. However, both the $[(FA-H)+Mg(Terpy)]^+$ and $[(FA-H)+Mg(Phen)]^+$ ions show prominent dissociation channels that lead to structurally uninformative product ions (see below), which leave room for improvement in the efficiency of informative product ion generation. This report describes the use of a commercially available ligand, 4,4′,4″-tri-tert-butyl-2,2′:6′,2″-terpyridine (ttb-Terpy), in generating divalent metal complexes for charge inversion reactions and compares the dissociation behaviors of $[FA-H+Mg(ttb-Terpy)]^+$ ions with the analogous $[(FA-H)+Mg(Terpy)]^+$ ions using various FA standards. The results demonstrate that superior performance is obtained using ttb-Terpy as the ligand for Mg^{2+}, at least for unsaturated and branched FAs as well as FAs with cyclopropane moieties.

2. EXPERIMENTAL SECTION

2.1 Nomenclature

We adopt the nomenclature for lipids recommended by the International Union of Pure and Applied Chemistry (IUPAC). Conventionally, the first carbon (C1) in the aliphatic chain is the carboxyl carbon. The shorthand notation used denotes the number of carbon atoms followed by the number of carbon−carbon double bonds, designated after the colon, and definitive double bond position(s) indicated inside parentheses. The shorthand notation 18:1 (9), for example, represents an 18-carbon chain FA with one double bond at position C9=C10. Where known, the stereochemistry of carbon−carbon double bonds is assigned as Z for *cis* and E for *trans.* For example, oleic acid is 18:1(9Z).[43,44,27,28]

2.2 Chemicals

Magnesium chloride, 2,2′:6′,2″-terpyridine (Terpy) and 4,4′,4″-tri-tert-butyl-2,2′:6′,2″-terpyridine (ttb-Terpy) were purchased from Millipore-Sigma (St. Louis, MO). Lipid standards; heptadecanoic acid (FA 17:0), 14-methyl palmitic acid (FA 16:0 (14Me)), 15-methyl palmitic acid (FA 16:0 (15 Me)) and Oleic acid (FA 18:1 (9Z)) were purchased from Cayman Chemical Company (Ann Arbor, MI). 1-palmitoyl-2-cis-9,10-methylenehexadecanoyl-sn-glycero-3-phosphocholine (16:0-17:0 cyclo PC) was obtained from Avanti Polar Lipids (Alabama, AL). HPLC-grade methanol, water, and chloroform were purchased from Fisher Scientific (Pittsburgh, PA).

2.3 Mass Spectrometry

All data, with the exception of the spectrum of **Figure S2**, were collected on modified a Sciex QTRAP 4000 hybrid triple quadrupole/linear ion trap mass spectrometer modified to enable ion-ion reactions. **Figure S2** was collected on a Sciex 5600 quadrupole time-of-flight previously modified for ion/ion reaction capabilities.[45] Briefly, alternately pulsed nano-electrospray

ionization (nESI) was used for analyte and reagent ion generation.[46,29,30,31] Deprotonated fatty acids, [FA - H]-, were generated via negative ion mode nESI, mass selected during transit through Q1, and transferred to q2 for storage. To generate fatty acid anions from 16:0-17:0 cyclo PC, direct infusion negative ion nESI was first used to generate the lipid anion, then the anion was isolated during transit through Q1 and sent to the high-pressure collision cell, q2. Collisional activation of the lipid anion in q2 was employed to generate the fatty acyl carboxylate anion, $[FA - H]^-$. Next, the charge inversion reagent, doubly charged magnesium tri-tert-butyl-terpyridine complex cations, denoted $[Mg(ttb\text{-}Terpy)_2]^{2+}$ or magnesium terpyridine complex cations, denoted $[Mg(Terpy)_2]^{2+}$, were generated via positive ion mode nESI. To facilitate the ion/ion reaction, magnesium complex dications and lipid anions were mutually stored in q2 for 300ms, resulting in the formation of charge-inverted lipid cations $[FA - H + Mg(L)]^+$, where L = Terpy or ttb-Terpy. The charge inverted product, $[FA\text{-}H + Mg(L)]^+$ was transferred to and isolated in Q3 prior to ion-trap CID. Product ions and residual precursor ions, if present, were then analyzed via mass selective axial ejection.[47]

3. RESULTS AND DISCUSSION

3.1 Saturated straight-chain fatty acids

The experimental sequences of reactions used for comparing the reagent cations $[Mg(ttb\text{-}Terpy)_2]^{2+}$ (right) and $[Mg(Terpy)_2]^{2+}$ (left) for generating structural information from a fatty acid anion are shown in **Scheme 1**. The overall efficiency for the conversion of analyte ions to structurally informative product ions is determined by the combined efficiencies of steps 1 and 2 in **Scheme 1**. Step 1 is the ion/ion reaction between $[Mg(L)_2]^{2+}$ and $[FA\text{-}H]^-$. Given the highly exoergic nature of mutual neutralization and the absence of a dielectric medium, essentially all ion/ion reactions in the gas-phase are unit efficient (i.e., a reaction occurs upon every collision).[48] As a result, as long as there is an excess of reagent ions and sufficient reaction time is allowed, 100% of the analyte ions will react. Such conditions are usually straightforward to achieve. Gas-phase ion/ion reactions can occur via the transfer of a small charged particle (e.g., an electron or proton) at a crossing point on the potential energy surface or via a long-lived complex.[49,50] Charge inversion reactions are much more likely to take place via a long-lived complex than via multiple charge single charge transfers at a distance. In the case of the reaction of a singly-charged anion with a multiply-charged cation, as in the present case, a single electron transfer from the analyte to the reagent or a proton transfer from the reagent to the analyte results in analyte neutralization, which would constitute an ion loss channel. The positive ion mode post-ion/ion reaction spectra, however, show no evidence for either electron transfer to or proton transfer from the $[Mg(L)_2]^{2+}$ ions in this study (see **Figure S1** for an example), which would be apparent via the appearance of singly charged reagent ions or fragments therefrom. Step 1 for both reagents, therefore, can be 100% efficient provided an excess of reagent cations are used.

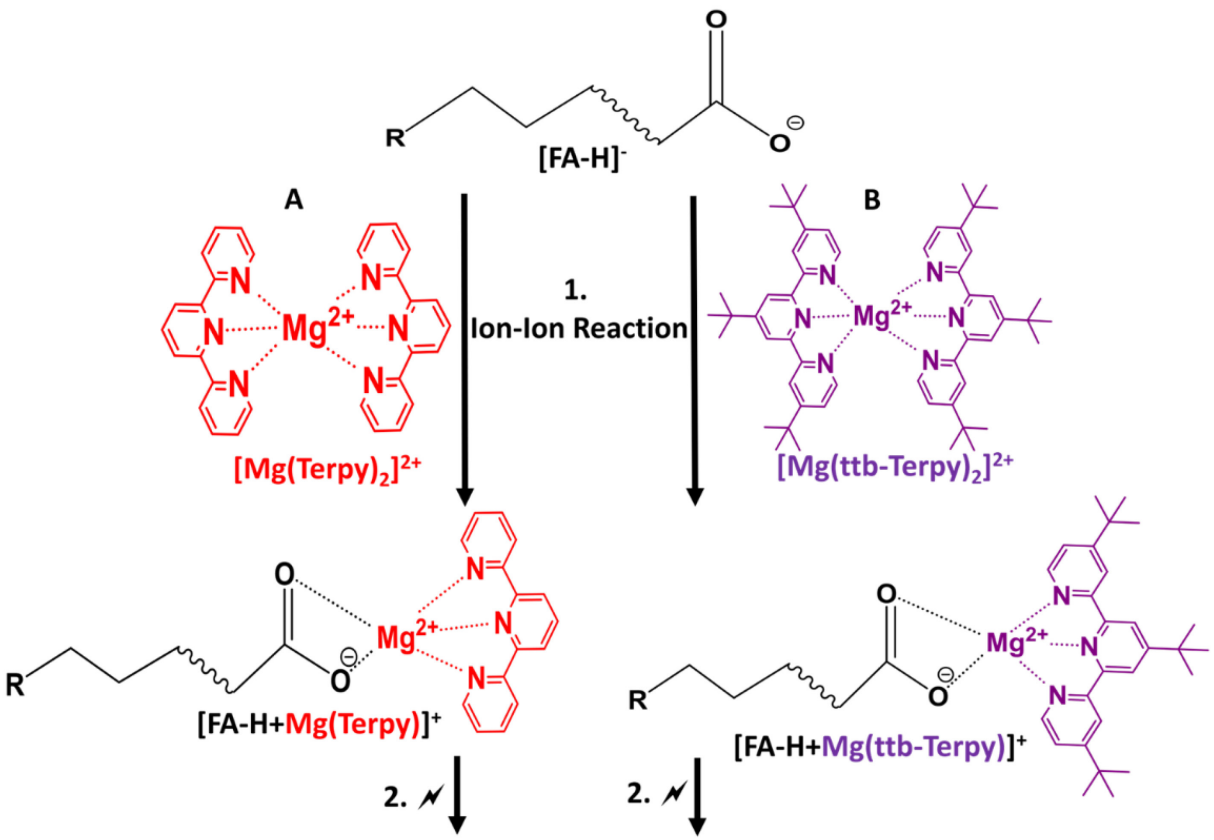

Scheme 1: Gas-phase charge inversion ion/ion reaction between $[FA - H]^-$ (right) and $[Mg(ttb\text{-}Terpy)_2]^{2+}$ for the generation of $[FA - H + Mg(ttb\text{-}Terpy)]^+$ ions and (left) $[Mg(Terpy)_2]^{2+}$ for the generation of $[FA - H + Mg(Terpy)]^+$.

Figure 1 compares ion trap CID (IT-CID) product ion spectra of $[FA\ 17:0 - H + Mg(Terpy)]^+$ (*m/z* 526) (**Figure 1a**) and $[FA\ 17:0 - H + Mg(ttb\text{-}Terpy)]^+$ (*m/z* 694) (**Figure 1b**). In each case, the base peak in the spectrum corresponds to the hydroxide of the metal-ligand (i.e., $HOMg(L)^+$). These ions are observed at *m/z* 274 ($HOMg(Terpy)^+$) and *m/z* 442 ($HOMg(ttb\text{-}Terpy)^+$), respectively. Both also show a series of peaks differing by 14 Da that reflect cleavage along the fatty acid chain. Similar dissociation behavior was originally reported via high energy CID of closed-shell fatty acid ions,[51] involving charge-remote fragmentation (CRF),[52,53,54] although the same products can also arise from radical-directed dissociation (RDD).[55,56] The fatty acid backbone cleavages constitute the structurally informative fragmentation channels whereas the metal-ligand hydroxide ions arise from parasitic channels that reduce the efficiency of step 2 in **Scheme 1**. It is clear from the comparison of **Figure 1** that CID of the $[FA\ 17:0 - H + Mg(ttb\text{-}Terpy)]^+$ ion yields at least an order of magnitude greater product ion abundance from lipid backbone cleavages relative to CID of the $[FA\ 17:0 - H + Mg(ttb\text{-}Terpy)]^+$ ion. That is, step 2 in the overall process in **Scheme 1** is much more efficient for generating lipid structural information when using $[Mg(ttb\text{-}Terpy)_2]^{2+}$ as the reagent ion relative to $[Mg(Terpy)_2]^{2+}$. It is also apparent that the high mass fragments that result from the loss of one or a few carbons from the end of the lipid chain are far more abundant upon CID of the $[FA\ 17:0 - H + Mg(ttb\text{-}Terpy)]^+$ ion relative

to CID of the [FA 17:0 – H + Mg(Terpy)]$^+$ ion. For example, the losses of 16 Da and 30 Da are far more abundant in **Figure 1b** than in **Figure 1a**. Note that the loss of 15 Da was also clearly apparent when the CID step was performed in q2 (see **Figure S2**) while it was not an abundant product when CID was performed in Q3. The main difference between the two collision regions is background pressure, with q2 operated in the range of 2-10 mtorr and Q3 operated in the range of 1-10x10^{-5} torr. The cooling rate is higher in q2, which tends to minimize sequential cleavages when single-frequency collisional activation is used.[57] This observation suggests that loss of a methyl radical is followed by sequential cleavage(s), which is supported further below.

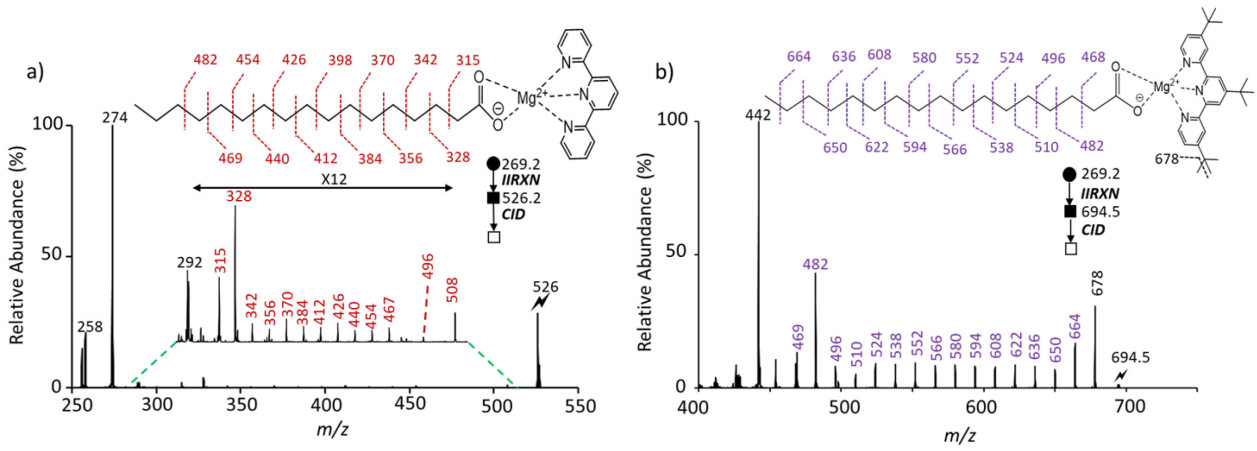

Figure 1: Ion trap CID product ion spectra of a) [FA 17:0 – H + Mg(Terpy)]$^+$ and b) [FA 17:0 – H + Mg(ttb-Terpy)]$^+$. Note that circles (●/○) indicate negative ion mode analysis, while squares (■/□) indicate positive ion mode analysis. Filled symbols indicate a mass-elected ion and open symbols represent scanned products.[58]

Given the presence of alkyl groups on ttb-Terpy, it is of interest to determine the extent to which some of the carbon loss observed in **Figure 1b** might arise from the ligand. For example, the series of fatty acid cleavages in **Figure 1b** appears to be shifted by one methylene group from the expected mass values. In the absence of any carbon loss from the ligand, the C2-C3 cleavage from the [FA 17:0 – H + Mg(ttb-Terpy)]$^+$ ion that is analogous to the *m/z* 315 product from the [FA 17:0 – H + Mg(Terpy)]$^+$ ion, which is the [•CH_2CO_2-H+Mg(Terpy)]$^+$ ion, should appear at *m/z* 483 for [•CH_2CO_2-H+Mg(ttb-Terpy)]$^+$. An abundant product is observed at *m/z* 482 while there is another abundant product at *m/z* 469 from [FA 17:0 – H + Mg(ttb-Terpy)]$^+$. This raises the question as to whether the *m/z* 469 and 482 peaks in **Figure 1b** are actually the product ions analogous to those represented by *m/z* 315 and 328 in **Figure 1a**. To address this question, perdeuterated 17:0 was ionized in the negative ion mode (33D exchanged for 33H in the deprotonated ion) and reacted with unlabeled Mg(ttb-Terpy)$_2^{2+}$. The IT-CID product ion spectrum of [17:0 d33-H+Mb(ttb-Terpy)]$^+$ (*m/z* 727) is shown in **Figure 2**. The base product ion peak arises from the loss of 16 Da, which is consistent with loss of CH_4 from the ligand. (The loss of 16 Da could, in principle, arise from the loss of CH_2D• or CD_2, both of which are highly unlikely.) There is also a loss of 30 Da, which is consistent with loss of C_2H_6 from the ligand, either as ethane

or two methyl radicals from the ligand. There are several plausible scenarios for the underlying processes associated with the cleavages along the FA backbone, which experiments with the labeled FA can distinguish. For example, if the methane and ethane losses from the ligand are simply side channels and the lipid backbone cleavages arise from CRF from the intact [17:0 d33-H+Mg(ttb-Terpy)]$^+$ ion, the predicted FA cleavages arehigh by 13 Da compared with the experimentally determined product ion masses in **Figure 2** (see **Table S1** for predicted masses from CRF of [17:0 d33-H+Mg(ttb-Terpy)]$^+$). Likewise, if the lipid backbone cleavages arise from sequential fragmentation beginning with methane loss from the ligand (i.e., from the [17:0 d33-H+Mg(ttb-Terpy – CH_4)]$^+$ ion, all of the predicted product ions are low by 3 Da (See **Table S1** for the predicted masses from CRF of [17:0 d33-H+Mg(ttb-Terpy – CH_4)]$^+$ ion). Hence, the labelling data indicates that CRF is not the likely process for the fatty acid backbone cleavages. Rather, if backbone cleavage arises from loss of CH_3• from the ligand, D• atom transfer from the FA chain to the ligand followed by RDD, all of the predicted FA cleavages line up with the measured masses of the product ions (see **Table S1** for the predicted masses from CID of [17:0 d33-D•-H+Mg(ttb-Terpy – CH_3• + D•)]$^+$). As noted above, direct evidence for loss of CH_3• is observed from CID in q2 but very little signal associated with CH_3• is observed via IT-CID in the lower pressure environment of Q3. The labelling results suggest that the first-generation loss of CH_3• is followed by subsequent D• atom transfer and facile radical-initiated cleavage. We also note that there is a relatively small signal associated with the loss of two carbon atoms with a nominal mass loss of 33 Da (*m/z* 694). The peak corresponds to an initial loss of CH_3•, D• atom from the FA chain, followed by loss of CD_3• from the end of the fatty acid chain, which is an expected channel via RDD (i.e., α-cleavage from a radical site at C15 of the FA chain resulting in a double bond between the initial C15 and C16 with loss of the C17 as a methyl radical). Hence, abundant products from cleavages of all C-C bonds in the fatty acid chain, with the exception of C1-C2, are observed. However, the labelling data indicates that most of the loss of 30 Da in **Figure 1b** arises from losses of both carbons from the ligand with only a minor contribution from sequential loss of CH_3• from the ligand followed by CH_3• loss from the end of the fatty acid chain.

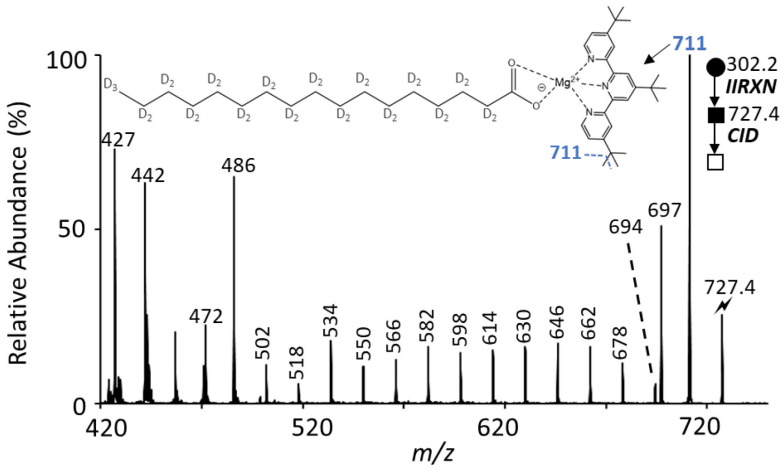

Figure 2: IT-CID product ion spectrum of [17:0 d33-H+Mg(ttb-Terpy)]$^+$. See **Figure 1** for description of the circles (●/○) and squares (■/□)**.**.

As indicated above, CRF from the [17:0 d33-H+Mg(ttb-Terpy – CH_4)]$^+$ ion (*m/z* 711 in **Figure 2**) is expected to give fatty acid backbone cleavages that differ in mass by 3 Da from the observed products (see **Table S1**). **Figure S3** shows the IT-CID spectrum of the [17:0 d33-H+Mg(ttb-Terpy – CH_4)]$^+$ ion. This ion also shows major losses of 16 Da (CH_4 loss) and 30 Da (loss of the elements of C_2H_6). It also shows evidence for the sequential loss of CH_3• from the ligand followed by CD_3• loss from the end of the fatty acid (*m/z* 694). Evidence for RDD cleavage at every C-C bond except C1-C2 is also present. As expected, each of the fatty acid backbone cleavage products appear 16 Da lower in mass than the corresponding fragment in **Figure 2** due to the fact that the ligand has lost a molecule of CH_4 (compare **Tables S1** and **S2**). This result provides confirmatory evidence that sequential cleavage beginning with the loss of CH_4 from [17:0 d33-H+Mg(ttb-Terpy)]$^+$ via CRF does not contribute to the spectrum of **Figure 1b**. Rather, loss of CH_3•, evidence for which is apparent in **Figure S3**, followed by D• transfer and RDD accounts for the observed masses of the product ions from fatty acid cleavage, as shown in **Scheme 2**.

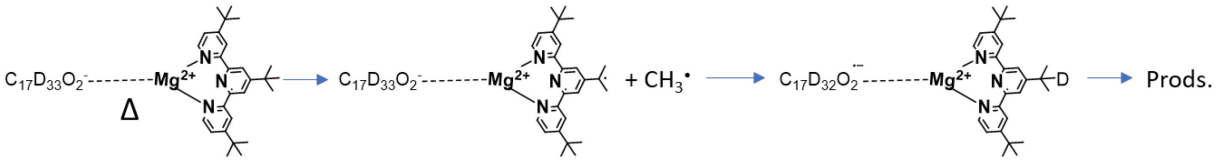

Scheme 2: Process leading to RDD of fatty acid ions, as revealed by labeling studies.

The bond dissociation energy (BDE) for cleavage of a $(CH_3)_3C$-CH_3 bond, which should approximate the energy requirement for methyl loss from the ligand side-chain here, is 87.5±0.4 kcal/mol.[59] Relevant fatty acid C-H BDEs are provided in **Table 1**. The relevant BDE for the tertiary radical generated upon methyl loss from the ligand is approximated by that for $(CH_3)_3C$-H, which is 96.5±0.4 kcal/mole. This is high enough to extract a hydrogen atom from an allylic carbon and from the methylene adjacent to the carboxylate (see Table 1), and should be close to that of a branching site in the fatty acid,

if present. Extraction of a hydrogen from the primary and secondary carbons of the fatty acid chain is expected to be endothermic by a few kcal/mol.

C-H bond	BDE_{298} (kcal/mol)
CH_3CH_2-H	101.1±0.4
$(CH_3)_2CH$-H	98.6±0.4
$(CH_3)_3C$-H	96.5±0.4
$(CH_3)(CO_2H)CH$-H[60]	94.3
CH_2CHCH_2-H	88.8±0.4

Table 1. List of homolytic bond dissociation energies at 298 K for C-H bond types relevant to this work.[59,60]

We note that both even- and odd-electron dissociation products should be formed in RDD. In most of the RDD literature involving fatty acid ions, the odd-electron products are not prominent and are often not observed. In recent work with a substituted Terpy ligand designed to generate a benzylic radical site on the ligand, which is a significantly more stable radical than any of the potential radical sites on the fatty acid, the expected odd-electron fragments could be observed under gentle IT-CID conditions but less so under higher amplitude activation conditions or beam-type collisional activation.[61] It was also demonstrated in that work that the odd-electron RDD products are significantly less stable than the even-electron counterparts and tend to fragment to even-electron higher generation dissociation products. The tertiary hydrocarbon radical site generated via CH_3• loss is more comparable in stability to the potential radical sites on the hydrocarbon portion of the fatty acid. We presume the low abundance of odd-electron products, with the exception of the fragment arising from cleavage of the bond between C2 and C3, is due to rapid sequential cleavage.

Figure 3 shows an expanded region of the IT-CID spectra of [FA 18:1 (9Z) – H + Mg(Terpy)]$^+$ generated using a 50 ms collisional activation period followed by (a) a 1 ms time delay prior to ejection of the *m/z* 256 ion and (b) a 60 ms storage period prior to ejection of the *m/z* 256 ion. At the shorter storage time, prominent product ions are observed from three small charged particle transfers (i.e., proton transfer from Mg(Terpy)$^{2+}$ to the lipid anion (*m/z* 256), electron transfer from the lipid to Mg(Terpy)$^{2+}$ (*m/z* 257), and hydride transfer from the lipid to Mg(Terpy)$^{2+}$ (*m/z* 258)). Note that the *m/z* 256 and 258 ions are both clearly apparent in **Figure 1a**. At the longer storage time, the ions at *m/z* 256, 257, and 258 decrease in abundance while the HOMg(Terpy)$_2^{2+}$ ion increases dramatically due to ion/molecule reactions involving water vapor present in the vacuum system.[62] Hence, most of the uninformative product ion signal in **Figure 1**, as represented by the HOMg(L)$^+$ peaks (m/z 274 for HOMg(Terpy)$^+$ and m/z 442 for HOMg(ttb-Terpy)$^+$, likely originates from the small charged-particle transfer processes followed by an ion/molecule reaction with water. (Note also that evidence for loss of a methyl group from ttb-Terpy is also apparent in the low *m/z* region of **Figures 1b** and **2**. For example, the *m/z* 427 ion corresponds in mass to [HOMg(ttb-Terpy) – CH_3•]$^+$. This suggests that small particle transfer can occur both before or after carbon loss from the ligand. Note also that the structurally

informative ions from cleavage of the lipid backbone are unreactive with water.) A major difference between the ion trap CID of [FA 17:0 – H + Mg(Terpy)]$^+$ and [FA 17:0 – H + Mg(ttb-Terpy)]$^+$ is that the small charged-particle transfer processes are significantly less competitive with the latter precursor ion relative to the former. We hypothesize that this can arise either from stabilization of the metal ion with respect to charged particle transfer due to the presence of the three t-butyl electron-donating groups or to methyl and methane loss being two facile channels from ttb-Terpy that more effectively compete with charged particle transfer, or both.

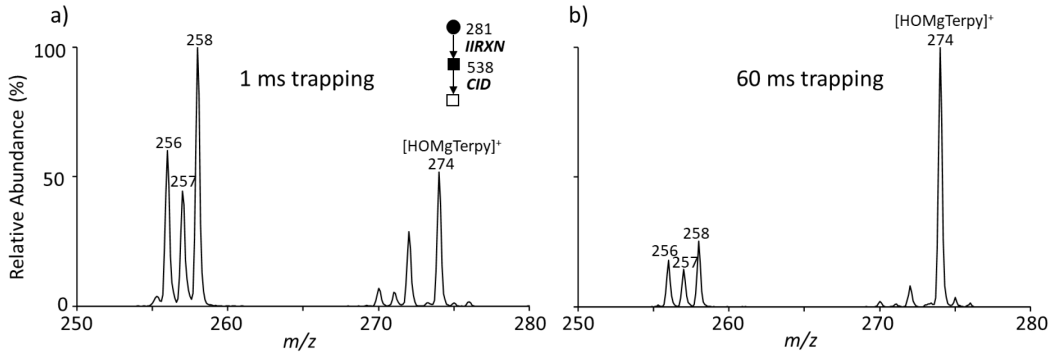

Figure 3: Ion trap CID spectra of [FA 18:1 (9Z) – H + Mg(Terpy)]$^+$ generated using a 50 ms collisional activation period followed by (a) a 1 ms storage period prior to mass analysis and (b) a 60 ms storage period prior to mass analysis. See **Figure 1** for description of the circles (●/○) and squares (■/□)**.**

3.2 Branched saturated fatty acids.

With the understanding of the major mechanisms involved in the IT-CID of the [FA-H+Mg(ttb-Terpy)]$^+$ ion, it is possible to correctly interpret the structural information present in the product ion spectrum. The location of branching, if present, in a saturated fatty acid is an example of an important structural characteristic of interest.[63,64,65,66,67,68] RDD has been demonstrated to be particularly useful in localizing branching sites.[23,58] A recent study has demonstrated how a combination of on-line liquid chromatography (LC) with charge-switching involving CID of [FA-H+Mg(Terpy)]$^+$ ion can distinguish isomeric iso-, anteiso-, and straight chains fatty acids.[41] However, the diagnostic signals in the IT-CID of the [FA-H+Mg(Terpy)]$^+$ ions are relatively low (see **Figure 4**) and the differences are subtle, which required the use of LC. **Figure 4** compares the IT-CID product ion spectra of the (**Figure 4a**) [FA 16:0 (14 Me) − H + Mg (Terpy)]$^+$ and (**Figure 4b**) [FA 16:0 (15 Me) – H +Mg(Terpy)]$^+$ ions with the corresponding spectra of (**Figure 4c**) [FA 16:0(14 Me) − H + Mg(ttb-Terpy)]$^+$ and (**Figure 4d**) [FA 16:0 (15 Me) − H + Mg (ttb-Terpy)]$^+$. Product ion spectra of the isomeric straight-chain ions are shown in **Figures 1a** and **1b**, respectively. As in the comparison of **Figure 1**, the fatty acid cleavage products in the product ion spectra of the [FA-H+Mg(ttb-Terpy)]$^+$ ions are in much greater relative abundance than those from the [FA-H+Mg(Terpy)]$^+$ ions. It is important to recognize that most of the signal associated with the losses of one (*m/z* 678) and two carbons (*m/z* 664) originated from losses from the ligand. However, with the added realization that the fatty acid fragments are formed via RDD and that the attached cation is of the form [Mg(ttb-Terpy) – CH_3• + H•)]$^{2+}$, the smallest fatty acid

fragment (i.e., [•CH_2CO_2-H+Mg(ttb-Terpy) – CH_3• + H•]$^+$) appears at *m/z* 469. The next fatty acid fragment (i.e., [CH_2=CHCO2-H+Mg(ttb-Terpy) – CH_3• + H•]$^+$ appears at *m/z* 482. The remaining fragments are spaced by 14 Da until the branching site is reached, where there is an obvious decrease in relative abundance. In the case of the [FA 16:0 (14 Me) − H + Mg (ttb-Terpy)]$^+$ ion, the decrease at *m/z* 636 indicates the branching site at C14 (see **Figure 4c**) whereas for the [FA 16:0 (15 Me) − H + Mg (ttb-Terpy)]$^+$ ion, the site of diminished signal appears at *m/z* 650 (see **Figure 4d**) indicating branching at C15.

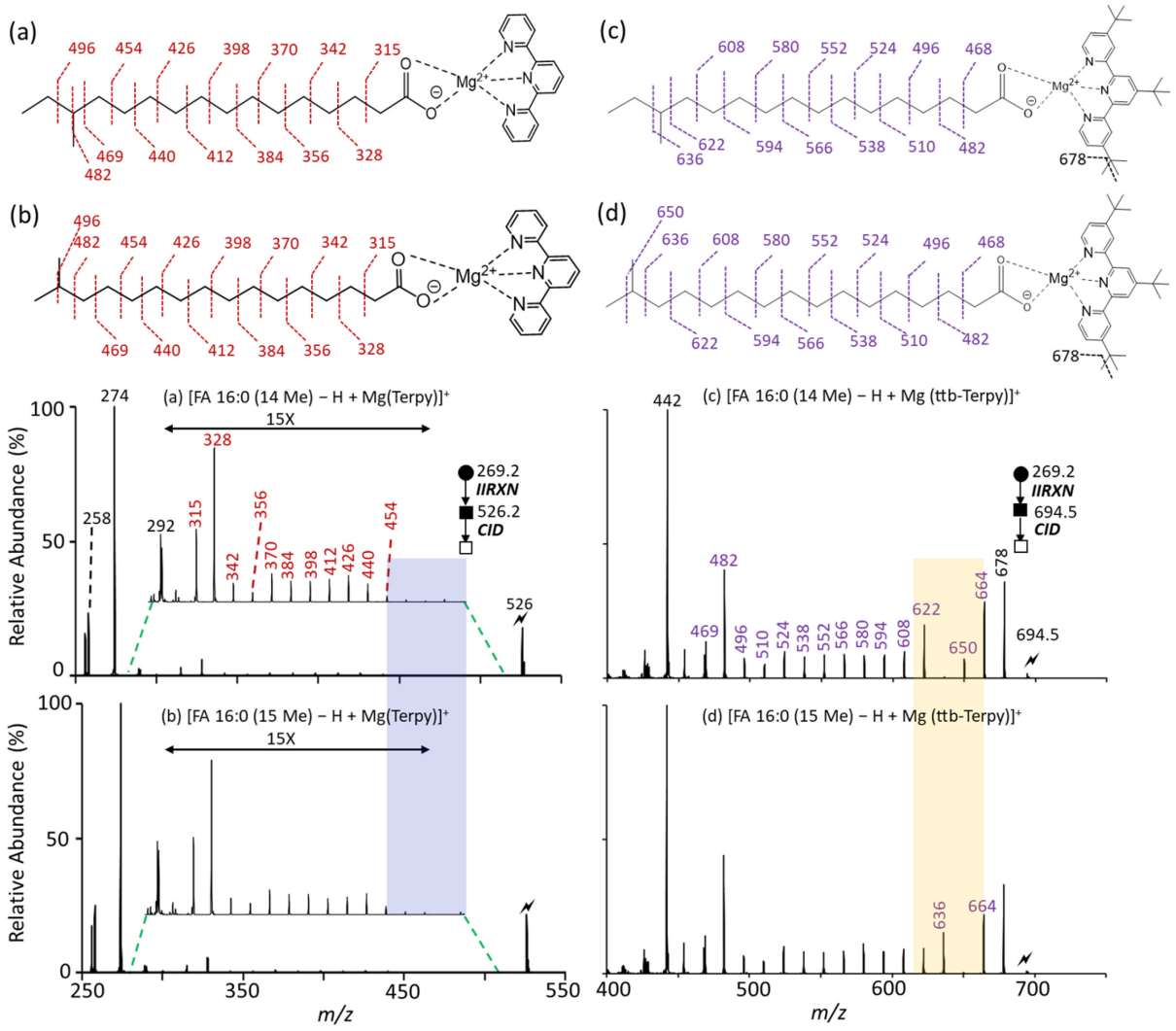

Figure 4: Ion-trap CID of (a) [FA 16:0 (14 Me) − H + Mg(Terpy)]$^+$ and (b) [FA 16:0 (15 Me) – H +Mg(Terpy)]$^+$ derived from the gas-phase ion/ion reaction of singly deprotonated [FA 16:0 (14 Me)-H]$^-$ and [FA 16:0 (15 Me)-H]$^-$ with [$Mg(Terpy)_2$]$^{2+}$. Ion-trap CID of (c) [FA 16:0(14 Me) − H + Mg(ttb-Terpy)]$^+$ and (d) [FA 16:0 (15 Me) − H + Mg (ttb-Terpy)]$^+$ derived from the gas-phase ion/ion reaction of singly deprotonated [FA 16:0 (14 Me)-H]$^-$ and [FA 16:0 (15 Me)-H]$^-$ with [Mg(ttb-$Terpy)_2$]$^{2+}$. See **Figure 1** for description of the circles (●/○) and squares (■/□).

3.3 Unsaturated fatty acids

The localization of sites of unsaturation in fatty acids and fatty acid esters is often an important objective in the characterization of lipid structures and multiple approaches have been developed for this purpose that involve, for example, condensed-phase derivatization reactions, alternate activation methods, etc. An early application of the gas-phase ion/ion reaction charge switching approach described here was the generation of $[FA\text{-}H + Mg(Phen)]^+$ ions, where Phen is 1,10-phenanthroline, from fatty acid anions via reaction with $Mg(Phen_3)^{2+}$.[36,37,39] IT-CID of unsaturated $[FA\text{-}H + Mg(Phen)]^+$ ions revealed information on site(s) of unsaturation via CRF mechanisms often used to rationalize fragmentation from fixed-charge FA ions.[69,70] **Figure 5a** shows the IT-CID of $[FA\ 18{:}1 - H + Mg(Terpy)]^+$, which is very similar to the data for $[FA\ 18{:}1 - H + Mg(Phen)]^+$ after accounting for the difference in mass between Phen and Terpy. Interestingly, the vertical scale does not need to be expanded to bring the most abundant CID products from FA cleavage to the same scale as the $HOMg(Terpy)^+$ ion (*m/z* 274), as is the case with the saturated FA (see **Figure 1a**). Perhaps the double bond interacts with the metal to stabilize it with respect to small particle charge transfer. In any case, the higher m/z FA cleavage products remain of quite low relative abundance. The location of the double bond is apparent from product ion spectrum via the appearance of a so-called 'spectral gap', which is highlighted by the shaded region in **Figure 5a**. In general, the proximal (i.e., closest to the carboxylate group) allylic C-C cleavage generates a characteristic terminally unsaturated CRF ion, whereas the distal allylic C-C cleavage generates a doublet comprised of a CRF ion and a terminally saturated product ion. This tendency is prominent with the ttb-Terpy ligand as shown in the insert of **Figure 5a**. The observed spectral gap is the result of a dramatic suppression in product ion abundance of product ions representing the C=C double bond and the C-C cleavages vinylic to the double bond.

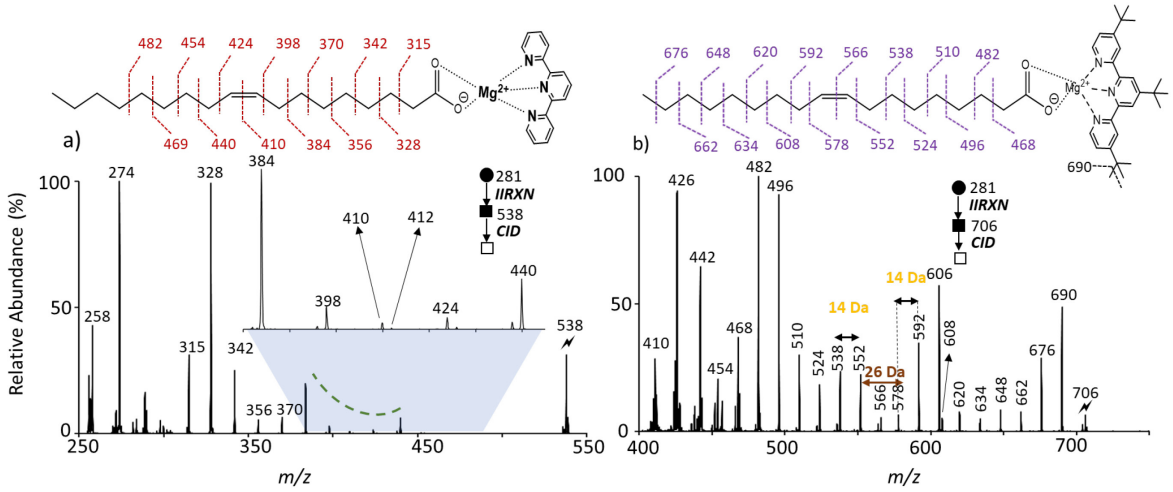

Figure 3: Ion-trap CID of (a) $[FA\ 18{:}1(9Z) - H + Mg(Terpy)]^+$ and (b) $[FA\ 18{:}1(9Z) - H + Mg(ttb\text{-}Terpy)]^+$ derived from the gas-phase ion/ion reaction of singly deprotonated $[FA\ 18{:}1(9Z) - H]^-$ with $[Mg(Terpy)_2]^{2+}$ and of $[Mg(ttb\text{-}Terpy)_2]^{2+}$, respectively. See **Figure 1** for description of the circles (●/○) and squares (■/□).

Figure 5b shows the IT-CID product ion spectrum of [FA 18:1(9Z) - H + Mg(ttb-Terpy)]$^+$. It is important to recognize that the fatty acid backbone cleavage products are formed after methyl radical loss from the ligand and hydrogen transfer from the fatty acid to the ligand via RDD mechanisms.[17,58] There is a spectral dip at the site of unsaturation in **Figure 5b**, in analogy with the behavior noted in **Figure 5a**. Furthermore, the region of diminished cleavage is centered at the transition between the 14 Da spacings associated with cleavages between adjacent saturated carbon atoms before and after the double bond. To illustrate, the 14 Da spacings between the C7-C8 and C10-C11 bonds are indicated in **Figure 5b** along with the 26 Da spacing between the fragments terminated by C8 and C10. Another example using FA 18:1(6Z) is shown in **Figure S4**.

3.4 Cyclopropane Fatty Acids (CPAs)

Cyclopropane moieties are commonplace in FAs and FAEs of bacteria[71,72,73] and are isomeric with unsaturated species of the same carbon number. The gas-phase ion/ion charge inversion process involving $Mg(Phen)_3^{2+}$ as the reagent ion has been demonstrated to be able to localize cyclopropane groups in the fatty acyl chains of cardiolipins[74] and glycerophospholipids[40] via IT-CID of $[FA\text{-}H + Mg(Phen)]^+$ ions. **Figure 6a** shows the IT-CID of [FA 17:0 (c9) − H + Mg (Terpy)]$^+$ (*m/z* 524), which is very similar to the data for [FA 17:0 (c9) − H + Mg (Terpy)]$^+$ after accounting for the difference in mass between Phen and Terpy. The signature for the presence of a cyclopropane group is the appearance of doublets associated with competing dissociation channels involving the ring,[40] which appear at C9. In this case, the fatty acyl chain was generated from fragmentation of an anion derived from a phosphatidylcholine (PC) standard, PC 16:0-17:0(c9). **Figure 6b** shows the IT-CID product ion spectrum of [FA 17:0 (c9) − H + Mg(ttb-Terpy)]$^+$ (*m/z* 692). As described above, the structurally informative product ions are formed via RDD following methyl radical loss from the ligand and the transfer of a hydrogen atom to the ligand. As in the previous examples, the first major fatty acid fragment appears at *m/z* 469 ($[\bullet CH_2CO_2\text{-}H+Mg(ttb\text{-}Terpy) - CH_3\bullet + H\bullet]^+$) with the first abundant even-electron product ($[CH_2{=}CHCO2\text{-}H+Mg(ttb\text{-}Terpy)$ at *m/z* 482. A series of products ions are spaced at 14 Da intervals until the pattern is interrupted at C9. The spacing between the most abundant peaks at C9 and C10 is 12 Da. The 14 Da spacing pattern resumes at C10. The region that separates the regular 14 Da spacings at the lower and higher masses localizes the site of the cyclopropyl group.

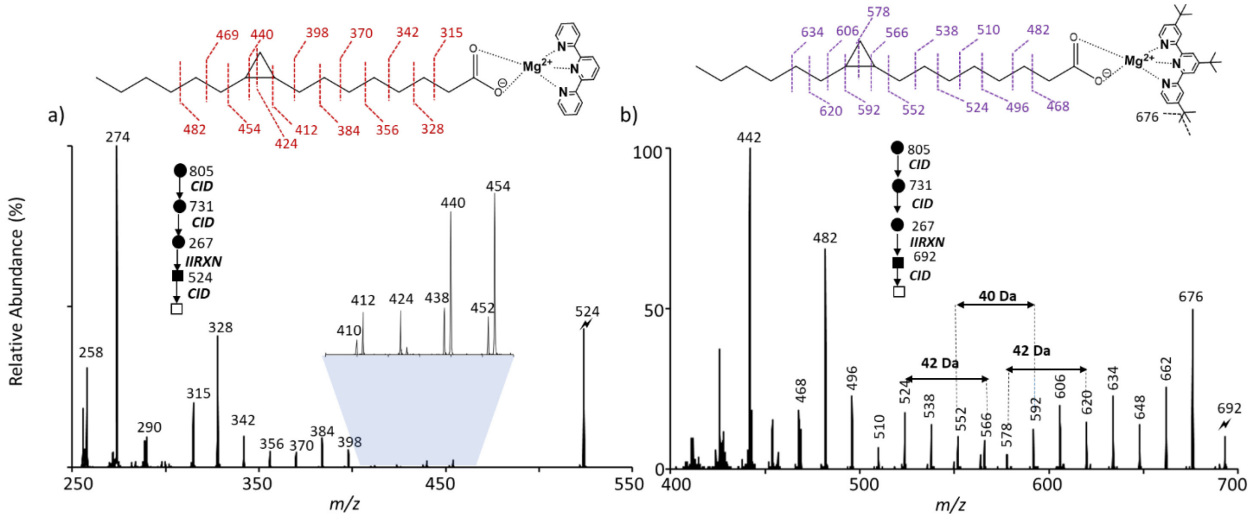

Figure 6: Ion-trap CID of (a) [FA 17:0 (c9) − H + Mg(Terpy)]$^+$ and (ii) [FA 17:0 (c9) − H + Mg (ttb-Terpy)]$^+$ derived from the gas-phase ion/ion reaction of singly deprotonated [FA 17:0(c9)-H]$^-$ with [Mg(Terpy)$_2$]$^{2+}$ and [Mg (ttb-Terpy)$_2$]$^{2+}$, respectively. See **Figure 1** for description of the circles (●/○) and squares (■/□).

CONCLUSIONS

The structural characterization of fatty acid anions, either generated directly or via fragmentation of a fatty acid ester-containing lipid, is facilitated via charge inversion with divalent metal-ligand complexes. Specifically, the use of Mg(Phen)$_3^{2+}$ or Mg(Terpy)$_2^{2+}$ leads to analyte ions of the form [FA-H + Mg(Phen or Terpy)]$^+$ that, upon IT-CID, fragment via charge remote mechanisms to give structural information. However, parasitic small charged-particle transfer processes compete with the structurally diagnostic cleavages, often carrying away most of the product ion charge. The use of ttb-Terpy as the ligand in the reagent complex (i.e., Mg(ttb-Terpy)$_2^{2+}$), on the other hand, leads to [FA-H + Mg(ttb-Terpy)]$^+$ ions that fragment much more extensively into structurally diagnostic products. Labeling studies showed that the major process underlying the formation of structurally diagnostic products is the loss of a methyl radical, hydrogen atom transfer from the fatty acid to the ligand, and subsequent RDD. While it is possible to localize double bonds, branching, and cyclopropane location using either Mg(Terpy)$_2^{2+}$ or Mg(ttb-Terpy)$_2^{2+}$ ions, the major dissociation mechanisms, CRF versus RDD, differ. For the direct comparisons shown here, the efficiency in generating the structural information of interest is significantly greater with Mg(ttb-Terpy)$_2^{2+}$. While further work relevant to other lipid classes is warranted to assess Mg(ttb-Terpy)$_2^{2+}$ as a reagent for gas-phase charge switching for structural characterization, it is demonstrated here to have attractive performance characteristics for fatty acid anions.

ACKNOWLEDGEMENTS

This research was supported by the National Science Foundation CHE-2304386. Dr. Hsi-Chun Chao is acknowledged for helpful advice and discussion. The authors also acknowledge SCIEX,

and particularly Mr. Frank Londry, for modifying the instruments to enable the ion/ion reaction experiments, and Dr. James W. Hager, also of SCIEX, for helpful discussions.

DATA AVAILABILITY STATEMENT

The data that support the findings of this study are available from the corresponding author upon reasonable request.

ORCID

Scott A. McLuckey - orcid.org/0000-0002-1648-5570; Email: mcluckey@purdue.edu

Supporting Information

Additional supporting information can be found online in the Supporting Information section at the end of this article.

AUTHOR INFORMATION

Corresponding Author

Scott A. McLuckey - Department of Chemistry, Purdue University, West Lafayette, Indiana 47907-2084, United States, orcid.org/0000-0002-1648-5570; Email: mcluckey@purdue.edu

Authors

Sarah T. Nsiah - Department of Chemistry, Purdue University, West Lafayette, Indiana 47907-2084, United States; Email: snsiah@purdue.edu

Kimberly C. Fabijanczuk – Department of Chemistry, Purdue University, West Lafayette, Indiana 47907-2084, United States; Email: kfabijan@purdue.edu

Credit Author Statement

Sarah T. Nsiah: Investigation, data curation, methodology, visualization, writing - original draft preparation. **Kimberly C. Fabijanczuk:** Investigation, data curation, methodology, visualization, writing – review and editing. **Scott A. McLuckey:** Methodology, resources, supervision, visualization, writing – review and editing.

Notes

The authors declare no competing financial interests.

References

1 Dowhan, W.; Bogdanov, M.; Mileykovskaya, E. Functional roles of lipids in membranes. Biochem. Lipids, Lipoproteins Membranes, 2008, 5th Rd., pp. 1-37.

2 Christie, W. W. Gas Chromatography-Mass Spectrometry Methods for Structural Analysis of Fatty Acids. *Lipids* **1998**; *33* (4), 343–353. https://doi.org/10.1007/s11745-998-0214-x

3 Zirrolli, J. A.; Murphy, R. C. Low-Energy Tandem Mass Spectrometry of the Molecular Ion Derived from Fatty Acid Methyl Esters: A Novel Method for Analysis of Branched-Chain Fatty Acids. *J Am Soc Mass Spectrom.* **1993**; *4* (3), 223–229. https://doi.org/10.1016/1044-0305(93)85085-C

4 Chiu, H.-H.; Kuo, C.-H. Gas Chromatography-Mass Spectrometry-Based Analytical Strategies for Fatty Acid Analysis in Biological Samples. *J Food Drug Anal.* **2020**; *28* (1), 60–73. https://doi.org/10.1016/j.jfda.2019.10.003

5 Wang, D. H.; Wang, Z.; Brenna, J. T. Gas Chromatography Chemical Ionization Mass Spectrometry and Tandem Mass Spectrometry for Identification and Straightforward Quantification of Branched Chain Fatty Acids in Foods. *J Agric Food Chem.* **2020**; *68* (17), 4973–4980. https://doi.org/10.1021/acs.jafc.0c01075

6 Pulfer, M.; Murphy, R.C. Electrospray mass spectrometry of phospholipids. Mass Spectrom Rev. **2003**; *22*(5) 332-364.

7 Wenk, M. R. The Emerging Field of Lipidomics. *Nat Rev Drug Discov.* **2005**; *4* (7), 594–610. https://doi.org/10.1038/nrd1776

8 Li, L.; Han, J.; Wang, Z.; Liu, J.; Wei, J.; Xiong, S.; Zhao, Z. Mass Spectrometry Methodology in Lipid Analysis. *Int J Mol Sci.* **2014**; *15* (6), 10492–10507. https://doi.org/10.3390/ijms150610492

9 Harkewicz, R.; Dennis, E. A. Applications of Mass Spectrometry to Lipids and Membranes. *Annu Rev Biochem.* **2011**; *80* (1), 301–325. https://doi.org/10.1146/annurev-biochem-060409-092612

10 Han, X. Multi-Dimensional Mass Spectrometry-Based Shotgun Lipidomics and the Altered Lipids at the Mild Cognitive Impairment Stage of Alzheimer's Disease. *Biochim Biophys Acta BBA -Mol Cell Biol Lipids.* **2010**; *1801* (8), 774–783. https://doi.org/10.1016/j.bbalip.2010.01.010

11 Han, X. Multi-Dimensional Mass Spectrometry-Based Shotgun Lipidomics and the Altered Lipids at the Mild Cognitive Impairment Stage of Alzheimer's Disease. *Biochim. Biophys. Acta BBA -Mol Cell Biol Lipids.* **2010**, *1801* (8), 774–783. https://doi.org/10.1016/j.bbalip.2010.01.010

12 Hsu, F. F. Mass Spectrometry-Based Shotgun Lipidomics – a Critical Review from the Technical Point of View. *Anal Bioanal Chem.* **2018**; *410* (25), 6387–6409. https://doi.org/10.1007/s00216-018-1252-y

13 Yang, K.; Zhao, Z.; Gross, R. W.; Han, X. Identification and Quantitation of Unsaturated Fatty Acid Isomers by Electrospray Ionization Tandem Mass Spectrometry: A Shotgun

Lipidomics Approach. *Anal Chem.* **2011**; *83* (11), 4243–4250. https://doi.org/10.1021/ac2006119

14 Blanksby, S. J.; Mitchell, T. W. Advances in Mass Spectrometry for Lipidomics. *Ann Rev Anal Chem.* **2010**; *3*, 433–467. https://doi.org/10.1146/annurev.anchem.111808.073705

15 Cao, W.; Cheng, S.; Yang, J.; Feng, J.; Zhang, W.; Li, Z.; Chen, Q.; Xia, Y.; Ouyang, Z.; Ma, X. Large-Scale Lipid Analysis with C=C Location and Sn-Position Isomer Resolving Power. *Nat Commun.* **2020**; *11* (1), 1–11. https://doi.org/10.1038/s41467-019-14180-4

16 Williams, P. E.; Klein, D. R.; Greer, S. M.; Brodbelt, J. S. Pinpointing Double Bond and Sn-Positions in Glycerophospholipids via Hybrid 193 NM Ultraviolet Photodissociation (UVPD) Mass Spectrometry. *J Am Chem Soc.* **2017**; *139* (44), 15681–15690. https://doi.org/10.1021/jacs.7b06416

17 Pham, H. T.; Trevitt, A. J.; Mitchell, T. W.; Blanksby, S. J. Rapid Differentiation of Isomeric Lipids by Photodissociation Mass Spectrometry of Fatty Acid Derivatives. *Rapid Commun Mass Spectrom.* **2013**; *27* (7), 805–815. https://doi.org/10.1002/rcm.6503

18 Thomas, M. C.; Mitchell, T. W.; Blanksby, S. J. Ozonolysis of Phospholipid Double Bonds during Electrospray Ionization: A New Tool for Structure Determination. *J Am Chem Soc.* **2006**; *128* (1), 58–59. https://doi.org/10.1021/ja056797h

19 Poad, B. L. J.; Zheng, X.; Mitchell, T. W.; Smith, R. D.; Baker, E. S.; Blanksby, S. J. Online Ozonolysis Combined with Ion Mobility-Mass Spectrometry Provides a New Platform for Lipid Isomer Analyses. *Anal. Chem.* **2018**; *90* (2), 1292–1300. https://doi.org/10.1021/acs.analchem.7b04091

20 Baba, T.; Campbell, J.L.; Le Blanc, Y.C.Y.; Baker, P.R.S.; Ikeda, K. Quantitative structural multiclass lipidomics using differential mobility: electron impact excitation of ions from organics (EIEIO) mass spectrometry. *J Lipid Research.* **2018**; *59*, P910-919.

21 Li, P.; Jackson, G.P. Charge transfer dissociation of phosphocholines: gas-phase ion/ion reactions between helium cations and phospholipid cations. *J. Mass Spectrom.* **2017**; *52*, 271-282.

22 Deimler, R.E.; Sander, M.; Jackson, G.P. Radical-induced fragmentation of phospholipid cations using metastable atom-activated dissociation mass spectrometry (MAD-MS). *Int J Mass Spectrom.* **2015**; *390*, 178-186.

23 Jian, R.; Zhao, X.; Lin, Q.; Xia, Y. Profiling of Branched-Chain Fatty Acids via Nitroxide Radical-Directed Dissociation Integrated on an LC-MS/MS Workflow. *Analyst.* **2022**; *147*, 2115–2123. https://doi.org/10.1039/d2an00266c

24 Young, R. S. E.; Flakelar, C. L.; Narreddula, V. R.; Jekimovs, L. J.; Menzel, J. P.; Poad, B. L. J.; Blanksby, S. J. Identification of Carbon-Carbon Double Bond Stereochemistry in

Unsaturated Fatty Acids by Charge-Remote Fragmentation of Fixed-Charge Derivatives. *Anal Chem.* **2022**; *94* (46), 16180–16188. https://doi.org/10.1021/acs.analchem.2c03625

25 Zhang, W.; Jian, R.; Zhao, J.; Liu, Y.; Xia, Y. Deep-Lipidotyping by Mass Spectrometry: Recent Technical Advances and Applications. *J. Lipid Res.* **2022**, *63* (7), 100219. https://doi.org/10.1016/j.jlr.2022.100219

26 Tang, S.; Cheng, H.; Yan, X. On-Demand Electrochemical Epoxidation in Nano-Electrospray Ionization Mass Spectrometry to Locate Carbon-Carbon Double Bonds. *Angew Chem Int Ed*. **2020**; *59*, 209-214.

27 Tang, S.; Chen, X.; Ke, Y.; Wang, F.; Yan, X. Voltage-Controlled Divergent Cascade of Electrochemical Reactions for Characterization of Lipids at Multiple Isomer Levels Using Mass Spectrometry. *Anal Chem.* **2022**; *94* (37), 12750–12756. https://doi.org/10.1021/acs.analchem.2c02375

28 Ma, X.; Xia, Y. Pinpointing Double Bonds in Lipids by Paternó-Büchi Reactions and Mass Spectrometry. Angew Chem Int Ed. **2014**, *53*, 2592-2596. doi.org/10.1002/anie.201310699

29 Randolph, C.E.; Blanksby, S.J.; McLuckey, S.A. Enhancing detection and characterization of lipids using charge manipulation in electrospray ionization-tandem mass spectrometry. *Chem Phys Lipids.* **2020**, *232*, 104970.

30 Yang, W.C.; Adamec, J.; Regnier, F. Enhancement of the LC/MS analysis of fatty acids through derivatization and stable isotope coding. *Anal Chem.* **2007**; *79* (14), 5150–5157.

31 Bollinger, J. G.; Rohan, G.; Sadilek, M.; Gelb, M. H., LC/ESI-MS/MS detection of FAs by charge reversal derivatization with more than four orders of magnitude improvement in sensitivity. *J Lipid Res.* **2013,** *54* (12), 3523-3530.

32 Yang, K.; Dilthey, B. G.; Gross, R. W., Identification and Quantitation of Fatty Acid Double Bond Positional Isomers: A Shotgun Lipidomics Approach Using Charge-Switch Derivatization. *Anal Chem.* **2013**; *85* (20), 9742-9750.

33 Wang, M.; Han, R. H.; Han, X. L., Fatty Acidomics: Global Analysis of Lipid Species Containing a Carboxyl Group with a Charge-Remote Fragmentation-Assisted Approach. *Anal Chem.* **2013**; *85* (19), 9312-9320.

34 Liu, X. P.; Moon, S. H.; Mancuso, D. J.; Jenkins, C. M.; Guan, S. P.; Sims, H. F.; Gross, R. W., Oxidized fatty acid analysis by charge-switch derivatization, selected reaction monitoring, and accurate mass quantitation. *Anal Biochem.* **2013**; *442* (1), 40-50.

35 Svane, S.; Gorshkov, V.; Kjeldsen, F. Charge Inversion of Phospholipids by Dimetal

Complexes for Positive Ion-Mode Electrospray Ionization Mass Spectrometry Analysis. *Anal Chem.* **2015**; *87* (17), 8732–8739. doi.org/10.1021/acs.analchem.5b01536

36 Randolph, C. E.; Foreman, D. J.; Betancourt, S. K.; Blanksby, S. J.; McLuckey, S. A. Gas-Phase Ion/Ion Reactions Involving Tris-Phenanthroline Alkaline Earth Metal Complexes as Charge Inversion Reagents for the Identification of Fatty Acids. *Anal Chem.* **2018**; *90* (21), 12861–12869. https://doi.org/10.1021/acs.analchem.8b03441.

37 Randolph, C. E.; Blanksby, S. J.; McLuckey, S. A. Toward Complete Structure Elucidation of Glycerophospholipids in the Gas Phase through Charge Inversion Ion/Ion Chemistry. *Anal Chem.* **2020**; 92(1), 1219-1227. https://doi.org/10.1021/acs.analchem.9b04376

38 Chao, H. C.; McLuckey, S. A. Differentiation and Quantification of Diastereomeric Pairs of Glycosphingolipids Using Gas-Phase Ion Chemistry. *Anal Chem.* **2020**; *92* (19), 13387–13395. https://doi.org/10.1021/acs.analchem.0c02755.

39 Randolph, C. E.; Foreman, D. J.; Blanksby, S. J.; Mcluckey, S. A. Generating Fatty Acid Profiles in the Gas Phase: Fatty Acid Identification and Relative Quantitation Using Ion/Ion Charge Inversion Chemistry. *Anal Chem.* **2019**; *91(14)*, 9032-9040. https://doi.org/10.1021/acs.analchem.9b01333

40 Shenault, D.M.; McLuckey, S.A.; Franklin, E.T. Localization of Cyclopropyl Groups and Alkenes Within Glycerophospholipids Using Gas-Phase Ion/Ion Chemistry. *J Mass Spectrom.* **2023**; *58*, e4913. https://doi.org/10.1002/jms.4913

41 Randolph, C. E.; Beveridge, C. H.; Iyer, S.; Blanksby, S. J.; McLuckey, S. A.; Chopra, G. Identification of Monomethyl Branched-Chain Lipids by a Combination of Liquid Chromatography Tandem Mass Spectrometry and Charge-Switching Chemistries. *J Am Soc Mass Spectrom.* **2022**; *33* (11), 2156–2164. https://doi.org/10.1021/jasms.2c00225

42 Chao, H.-C.; McLuckey, S.A. Recent Advances in Gas-phase Ion/ion Chemistry for Lipid Analysis. *Trends Anal Chem.* **2023**; *158*, 116852.

43 Fahy, E.; Subramaniam, S.; Murphy, R. C.; Nishijima, M.; Raetz, C. R. H.; Shimizu, T.; Spener, F.; Van Meer, G.; Wakelam, M. J. O.; Dennis, E. A. Update of the LIPID MAPS Comprehensive Classification System for Lipids. *J Lipid Res.* **2009**; *50* (SUPPL.), S9–S14. https://doi.org/10.1194/jlr.R800095-JLR200.

44 Liebisch, G.; Vizcaíno, J. A.; Köfeler, H.; Trötzmüller, M.; Griffiths, W. J.; Schmitz, G.; Spener, F.; Wakelam, M. J. O. Shorthand Notation for Lipid Structures Derived from Mass Spectrometry. *J Lipid Res.* **2013**; *54* (6), 1523–1530. https://doi.org/10.1194/jlr.M033506.

45 Bhanot, J.S.; Fabijanczuk, K.C.; Abdillahi, A.M.; Chao, H.-C.; Pizzala, N.J.; Londry, F.A.; Dziekonski, E.T.; J.W. Hager, J.W. Scott A. McLuckey, S.A. Adaptation and Operation of a Quadrupole/Time-of-Flight Tandem Mass Spectrometer for High Mass Ion/Ion Reaction Studies. *Int. J. Mass Spectrom.* **2022**; *478*, 116874.

46 Xia, Y.; Liang, X.; McLuckey, S. A. Pulsed Dual Electrospray Ionization for Ion/Ion Reactions. *J Am Soc Mass Spectrom.* **2005**; *16*, 1750-1756. https://doi.org/10.1016/j.jasms.2005.07.013

47 Londry, F.A.; Hager, J.W. Mass selective axial ejection from a linear quadrupole ion trap. *J Am Soc Mass Spectrom.* **2003**; *14(10)*, 1130-1147.

48 McLuckey, S.A.; Stephenson, Jr., J.L.; Asano, K.G. Ion/ion Proton Transfer Kinetics: Implications for Analysis of Ions Derived from Electrospray of Protein Mixtures. *Anal Chem.* **1998**; *70*, 1198-1202.

49 Wells, J.M.; Chrisman, P.M.; McLuckey, S.A. Formation and Characterization of Protein-protein Complexes in Vacuo. *J Am Chem Soc.* **2003**; *125*, 7238-7249.

50 Gunawardena, H.P.; He, M.; Chrisman, P.A.; Pitteri, S.J.; Hogan, J.M.; Hodges, B.D.M.; McLuckey, S.A. Electron Transfer versus Proton Transfer in Gas-Phase Ion-Ion Reactions of Polyprotonated Peptides. *J Am Chem Soc.* **2005**; *127*, 12627-12639. DOI: 10.1021/ja0526057

51 Jensen, N.J.; Tomer, K.B.; Gross, M.L. Gas-Phase Ion Decompositions Occurring Remote to a Charge Site. *J Am Chem Soc.* **1985**; *107*, 1863-1868.

52 Jensen, N.J.; Gross, M.L. Mass spectrometry methods for structural determination and analysis of fatty acids. *Mass Spectrom Rev.* **1987**, *6*, 497-536.

53 Gross, M. L. Charge-Remote Fragmentation: An Account of Research on Mechanisms and Applications. *Int J Mass Spectrom.* **2000**; *200* (1), 611–624. https://doi.org/10.1016/S1387-3806(00)00372-9.

54 Griffiths, W.J. Tandem Mass Spectrometry in the Study of Fatty Acids, Bile Acids, and Steroids. *Mass Spectrom Rev.* **2003**; *23*, 81-152.

55 Pham, H. T.; Julian, R. R. Characterization of Glycosphingolipid Epimers by Radical-Directed Dissociation Mass Spectrometry. *Analyst* **2016**; *141* (4), 1273–1278. https://doi.org/10.1039/C5AN02383A

56 Silzel, J. W., Julian, R. R. RDD-HCD Provides Variable Fragmentation Routes Dictated by Radical Stability. *J Am Soc Mass Spectrom.* **2023**; *34(3)*, 452–458. https://doi.org/10.1021/jasms.2c00326

57 Asano, K.G.; Goeringer, D.E.; Butcher, D.J.; McLuckey, S.A. Bath Gas Temperature and the Appearance of Ion Trap Tandem Mass Spectra of High-Mass Ions. *Int. J. Mass Spectrom.* **1999**; *190/191*, 281-293.

58 Schwartz, J.C.; Wade, A.P.; Enke, C.G.; Cooks, R.G. Systematic Delineation of Scan Modes in Multidimensional Mass Spectrometry. *Anal. Chem.* **1990**, *62*, 1809-1818.

59 Blanksby, S.J.; Ellison, G.B. Bond Dissociation Energies of Organic Molecules. *Acc. Chem. Res.* **2003**, *36*, 255-263.

60 Namysl, S.; Pelucchi, M.; Herbinet, O.; Frassoldati, A.; Faravelli, T.; Battin-Leclerc, F. A first evaluation of butanoic and pentanoic acid oxidation kinetics. *Chem. Eng. J.* **2019**, *373*, 973-984.

61 Shenault, D.M.; Fabijanczuk, K.C.; Murtada, R.; Finn, S.; Gonzalez, L.E.; Gao, J.; McLuckey, S.A. Gas-Phase Ion/Ion Reactions to Enable Radical Directed Dissociation of Fatty Acid Ions: Application to Localization of Methyl Branching. *Anal. Chem.*, In press. https://doi.org/10.1021/acs.analchem.3c04510

62 Fabijanczuk, K.C.; Altalhi, W.A.O.; Aldajani, A.M.O.; Canty, A.J.; McLuckey, S.A.; O'Hair, R.A.J. Ion-pairs as a Gateway to Transmetalation: Aryl Transfer from Boron to Nickel and Magnesium. *Dalton Transactions*. **2022**; *51*, 5699-5705. 10.1039/d2dt00746k

63 Kaneda, T. Iso- and Anteiso-Fatty Acids in Bacteria: Biosynthesis, Function, and Taxonomic Significance. *Microbiol Rev.* **1991**; *55* (2), 288–302.

64 Kniazeva, M.; Crawford, Q. T.; Seiber, M.; Wang, C.-Y.; Han, M. Monomethyl Branched-Chain Fatty Acids Play an Essential Role in Caenorhabditis Elegans Development. *PLoS Biol.* **2004**; *2* (9), e257. https://doi.org/10.1371/journal.pbio.0020257.

65 Wang, Z.; Wang, D. H.; Park, H. G.; Tobias, H. J.; Kothapalli, K. S. D.; Brenna, J. T. Structural Identification of Monounsaturated Branched Chain Fatty Acid Methyl Esters by Combination of Electron Ionization and Covalent Adduct Chemical Ionization Tandem Mass Spectrometry. *Anal Chem.* **2019**; *91* (23), 15147–15154. https://doi.org/10.1021/acs.analchem.9b03912.

66 Mostofian, B.; Zhuang, T.; Cheng, X.; Nickels, J. D. Branched-Chain Fatty Acid Content Modulates Structure, Fluidity, and Phase in Model Microbial Cell Membranes. *J Phys Chem B.* **2019**; *123* (27), 5814–5821. https://doi.org/10.1021/acs.jpcb.9b04326.

67 Ran-Ressler, R. R.; Devapatla, S.; Lawrence, P.; Brenna, J. T. Branched Chain Fatty Acids Are Constituents of the Normal Healthy Newborn Gastrointestinal Tract. *Pediatr Res.* **2008**; *64* (6), 605–609. https://doi.org/10.1203/PDR.0b013e318184d2e6.

68 Borchman, D.; Ramasubramanian, A. Human Meibum Chain Branching Variability with Age, Gender and Meibomian Gland Dysfunction. *Ocul Surf.* **2019**; *17* (2), 327–335. https://doi.org/10.1016/j.jtos.2018.12.005.

69 Frankfater, C.; Jian, X.; Hsu F.-F. Characterization of Long-Chain Fatty Acid as N-(4-Aminomethylphenyl) Pyridinium Derivative by MALDI LIFT-TOF/TOF Mass Spectrometry. *J Am Soc Mass Spectrom.* **2018**; *29(8)*, 1688-1699.

70 Wang, M.; Han, R.H.; Han, X. Fatty Acidomics: Global Analysis of Lipid Species Containing a Carboxyl Group with a Charge-Remote Fragmentation-Assisted Approach. *Anal Chem.* **2013**; *85*, 9312-9320.

71 Grogan, D.W.; Cronan, J.E. Cyclopropane Ring Formation in Membrane Lipids of Bacteria. *Microbiol Mol Biol Rev.* **1997**; *61* (4), 429–441.

72 Poger D, Mark AE. A Ring to Rule Them All: The Effect of Cyclopropane Fatty Acids on the Fluidity of Lipid Bilayers. *J Phys Chem B.* **2015**; *119* (17), 5487–5495. https://doi.org/10.1021/acs.jpcb.5b00958.

73 Zhang, Y.-M.; Rock, C.O. Membrane lipid homeostasis in bacteria. *Nat Rev Microbiol.* **2008**, *6*, 222–233. https://www.nature.com/articles/nrmicro1839

74 Randolph, C. E.; Shenault, D. S. M.; Blanksby, S. J.; Mcluckey, S. A. Localization of Carbon − Carbon Double Bond and Cyclopropane Sites in Cardiolipins via Gas-Phase Charge Inversion Reactions. J Am Soc Mass Spectrom. **2021**; 32(2), 455-464. https://doi.org/10.1021/jasms.0c00348